IOPscience iopscience.iop.org

Home Search Collections Journals About Contact us My IOPscience

Charge carrier transport in polyvinylcarbazole

This article has been downloaded from IOPscience. Please scroll down to see the full text article.

2006 J. Phys.: Condens. Matter 18 6365

(http://iopscience.iop.org/0953-8984/18/27/019)

View the table of contents for this issue, or go to the journal homepage for more

Download details:
IP Address: 129.252.86.83
The article was downloaded on 28/05/2010 at 12:15

Please note that terms and conditions apply.

INSTITUTE OF PHYSICS PUBLISHING JOURNAL OF PHYSICS: CONDENSED MATTER

J. Phys.: Condens. Matter **18** (2006) 6365–6377 doi:10.1088/0953-8984/18/27/019

Charge carrier transport in polyvinylcarbazole

Andrey P Tyutnev[1,3], Vladimir S Saenko[1], Evgenii D Pozhidaev[1] and Vladislav A Kolesnikov[2]

[1] Moscow State Institute of Electronics and Mathematics, Bolshoy Pereulok Trechsvyatitel. per., 3/12, Moscow, Russia
[2] Frumkin Institute of Physical Chemistry and Electrochemistry Russian Academy of Sciences, Leninskii prospekt, 31, Moscow, Russia

E-mail: aptyutnev@yandex.ru and fit@miem.edu.ru

Received 13 March 2006, in final form 30 May 2006
Published 23 June 2006
Online at stacks.iop.org/JPhysCM/18/6365

Abstract

A critical analysis of the existing time-of-flight (TOF) data in poly(*N*-vinylcarbazole) (PVK) proves that these are highly controversial with claims and counterclaims about charge carrier transport (dispersive versus Gaussian). It is felt that the TOF method taken alone is incapable of resolving the standing dilemma. As a final means to resolve it, we propose a combination of two varieties of the TOF technique using both sheet-like and uniform carrier generation modes in conjunction with radiation-induced conductivity measurements. All three techniques are realized using the ELA-50 electron gun facility. To demonstrate the effectiveness of our approach we report experimental data for PVK, which show that carrier transport in this polymer is indeed dispersive. Evidence is presented substantiating the gross interference the surface traps could exert on the shape of a TOF transient. As a result, a preflight part of the TOF signal should not be used for parameter evaluation.

1. Introduction

Poly(*N*-vinylcarbazole) (PVK) may be regarded as a model polymer (or a test ground) for all theories proposed so far to describe charge carrier transport in disordered organic solids. Indeed, two basic theories have been proposed to explain hole transport in it. First, there was the continuous-time random walk (CTRW) theory developed by Scher and Montroll [1]. It stressed the non-equilibrium (dispersive) transport implying that the average (effective) mobility of pulse-generated holes diminishes in time as $t^{-1+\alpha}$, with the so-called dispersive parameter α being less than 1.0. Later this formalism has been recovered in terms of the multiple trapping (MT) model [2].

[3] Author to whom any correspondence should be addressed.

An alternative approach has been put forward by Bässler [3, 4], emphasizing the quasi-equilibrium stage of the transport process. This has become known as the Gaussian disorder model (GDM).

As PVK is photoconductive it has been extensively investigated using the optical variant of the time of flight (TOF) technique. Experimental results differ with claims and counterclaims about charge carrier transport (dispersive versus Gaussian). The point of contention concerns the exact form of the TOF small signal current preceding the transit time t_{tr}. In the case of dispersive transport there is no clear-cut break marking this time which can only be found in a log j-versus-log t representation as the intersection of the initial ($t^{-1+\alpha}$) and final ($t^{-1-\alpha}$) asymptotes of the current.

The GDM predicts the appearance of a plateau with a clear break at t_{tr} followed by a short tail. The initial fall of the TOF current is understood in both models as reflecting the energy relaxation of charge carriers among localized states which arise as a result of breakdown of the long-range order in polymers. The completion of this process is marked by the onset of the plateau (GDM) while in the framework of MT the equilibration is never achieved.

The TOF technique as applied to disordered solids has one fundamental weakness already cited in literature [5, 6]. Unlike in single crystals, the role of surface traps in them is greatly enhanced. Because the TOF transient current decreases sharply with time any retarded release of surface-trapped carriers is bound to distort the trace, easily producing a shoulder or a cusp, or even a straight plateau as indicated in [6]. The effects of surface traps can easily explain the lack of uniformity as far as the form of the TOF signals is concerned.

Besides, there are other factors adding to the controversy. It follows from Gill's results that the large signal TOF transient features a cusp while in the small signal regime it reverts to one resembling dispersive signature [7] (this work was done before the very notion of the dispersive transport had been introduced, to say nothing of its theory).

Also, it has been shown that a specially deposited thin generation layer of amorphous Se on a PVK sample leads to the formation of a cusp on a TOF photocurrent even in the small signal regime [8].

In the meantime, detailed studies of triphenylamine (TFA) doped polyester undertaken by Pfister revealed that the preflight part of the TOF curve was often severely distorted such as to render parameter fitting using it totally inconclusive [9]. He even suggested discarding experimental curves exhibiting a plateau or a cusp as being grossly distorted, supposedly by surface traps. Accordingly, the post-transit part has been recommended for data reduction.

To eliminate all possible apprehensions about the quality of the experimental data we resorted to yet another variety of the TOF technique employing uniform ionization of the polymer (TOF-2).

Of course, TOF-2 fails to discriminate between electron and hole current contributions. Evidently, this presents no difficulty in systems with unipolar conduction such as PVK. Even in polymers featuring an ambipolar conduction it is rather more of a numerical than a fundamental nature. The main idea behind TOF-2 is to eliminate interface effects by producing a vast majority of carriers in the bulk. An important point to stress is that both techniques were used regularly in the past for studying electron mobility in liquids and gave consistent results [10].

Using radiation-induced conductivity (RIC) and analysing the current build-up curve greatly enhances the sensitivity of the method compared with both TOF techniques, which deal essentially with currents decaying following the pulse. This information may be used as an additional check in parameter fitting.

One beneficial factor of employing radiation based techniques is the fact that fast electrons unlike photons are known to have no ionization threshold and may serve as a universal means for producing charge carriers in polymers whether photoconductive or not.

The aim of the present paper is to establish the kind of transport which is operative in PVK, to demonstrate the limitations of the TOF technique as applied to disordered organic solids and finally prove the effectiveness of the proposed combination of methods (TOF-2, TOF and RIC) based on fast electrons as a universal ionizing means.

2. Theoretical basis for interpretation of experimental results

2.1. Dispersive transport

The best analytical approach to describe dispersive transport has been developed by Arkhipov and Rudenko [11, 12]. It is based on the concept of the τ-function and gives the closed-form description of the transient current for $0 \leqslant t \leqslant \infty$. These expressions are as follows:

TOF

$$j_{\delta s}(t) = (e\sigma_0/L)\frac{\mathrm{d}}{\mathrm{d}t}r(t)[1 - \exp(-L/r(t))] \tag{1}$$

TOF-2

$$j_{\delta v}(t) = e\sigma_0\frac{\mathrm{d}}{\mathrm{d}t}r^2(t)[r^{-1} + \exp(-r^{-1}) - 1], \tag{2}$$

and RIC

$$j_v(t) = \begin{cases} Leg_0 p(t), & t \leqslant t_0 \\ Leg_0[p(t) - p(t - t_0)], & t > t_0 \end{cases} \tag{3}$$

where $r(t) = \mu_0 F_0 \tau(t)/L$, $\tau(t) = \frac{\tau_0(\nu_0 t)^\alpha}{\alpha\gamma(\alpha,\nu_0 t)}$ and $\gamma(\alpha, x)$ is the incomplete gamma-function ($\gamma(\alpha, x) \to \Gamma(\alpha)$ for $x \to \infty$). Besides $p(t) = r^2(t)[r^{-1} + \exp(-r^{-1}) - 1]$, g_0 is the generation rate of charge carriers and t_0 is the pulse length. In the case of TOF-2 σ_0/L means the initial concentration of pulse-generated charge carriers.

Unfortunately, the above formulae are slightly inaccurate, and all the more so the larger the dispersion parameter. Thus, equation (1) gives

$$t_{\mathrm{tr}} = \nu_0^{-1}\left[\frac{\Gamma(1+\alpha)L}{\sqrt{2}\mu_0\tau_0 F_0}\right]^{1/\alpha}, \tag{4}$$

so that t_{tr} for the parameter values (slightly different from those of PVK) of figure 1 is equal to 148 ms. Graphic determination using Origin accessories gives 120 ms. This discrepancy underlines the inaccuracy associated with the extrapolation procedure inherently present in the transit time evaluation.

According to [11] the exact expression for t_{tr} is somewhat different:

$$t_{\mathrm{tr}} = \nu_0^{-1}\left[\frac{\Gamma^{3/2}(1+\alpha)\Gamma^{1/2}(1-\alpha)L}{\sqrt{2}\mu_0\tau_0 F_0}\right]^{1/\alpha}, \tag{5}$$

and the corrected transit time becomes 261 ms. Besides, the following relation holds ($\hat{t}_{\mathrm{tr}}$ is the TOF-2 transit time):

$$t_{\mathrm{tr}} = \left(\sqrt{3}\right)^{1/\alpha}\hat{t}_{\mathrm{tr}}. \tag{6}$$

For parameter evaluation we use equation (5). Similarly, to deal with RIC curves we rely on the exact formulae instead of what equation (3) gives in the limit of $t \ll \hat{t}_{\mathrm{tr}}$ for both $t \leqslant t_0$ (current build-up) and $t \geqslant 5t_0$ (current decay) [13]. Nevertheless, equations (1) and (2) are used to calculate the theoretical curves in all figures in this paper.

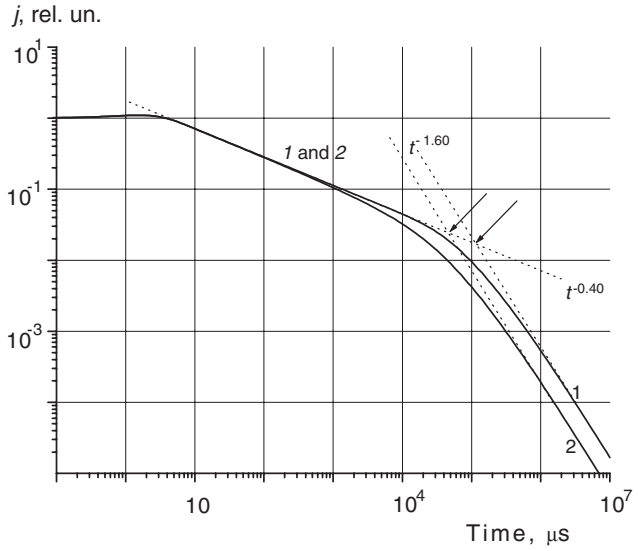

Figure 1. TOF (1) and TOF-2 (2) numerical curves in terms of MT theory. Model parameters $\alpha = 0.6$, $\mu_0\tau_0 = 0.5 \times 10^{-15}$ m^2 V^{-1}, $\nu_0 = 1 \times 10^6$ s^{-1}. Sample thickness 20 μm and electric field 2×10^7 V m^{-1}. The arrows indicate transit times determined graphically from computed curves. The TOF transit time t_{tr} as indicated by the right arrow is approximately equal to 120 ms; formula (4) gives 148 ms, while the exact expression (5) gives 261 ms. The corresponding figures for TOF-2 are as follows: 52.0, 59.1 and 104 ms. The initial plateau of both curves reflects the rather low value of the frequency factor. The current overshoot at early times is due to some inaccuracy of the τ-function formalism for $\alpha \geqslant 0.6$.

2.2. Gaussian transport

The GDM predicts that after some non-equilibrium phase the transport process attains the steady state and then proceeds as a normal Gaussian event with constant kinetic coefficients.

Accordingly, for $t \geqslant \tilde{t}$ (equilibration time) the TOF transient may be described by the classical expression [14]

$$j_(t) = \frac{\sigma_0 e \tilde{\mu} F_0}{L}\left[1 - \frac{1}{2}\mathrm{erfc}\left(\frac{L - \tilde{\mu}F_0 t}{\sqrt{4\tilde{D}t}}\right)\right]. \tag{7}$$

Here $\tilde{\mu}$ and $\tilde{D}$ are the quasi-equilibrium mobility and diffusion coefficient respectively, and $\mathrm{erfc}(x)$ is the complementary error function. For $t \geqslant 3t_{tr}$ the current decay is extremely fast:

$$j \propto 0.3\varsigma^{-1}\exp(-\varsigma^2) \tag{8}$$

where $\varsigma = \frac{\tilde{\mu}F_0 t - L}{2\sqrt{\tilde{D}t}}$. Thus, a TOF curve on a linear plot represents an initial spike followed by a plateau with a relatively short (and almost symmetrical about t_{tr}) tail. In the case of TOF-2 the plateau is replaced by a ramp. Thus, the expected change of the current form is rather drastic in going from the TOF to the TOF-2 technique. In contrast, the tails in a logarithmic plot are rather similar (figure 2).

A much more detailed picture of current behaviour is provided by analysing the GDM with the help of the percolation approach [15]. As a result, the hopping problem is effectively reduced to an MT problem with a Gaussian distribution of traps.

With the parameters used by Bässler for PVK [3, 4] (parameter of the cubic lattice 0.6 nm, inverse decay radius of the wavefunction 0.83×10^{10} m^{-1}, standard variance of

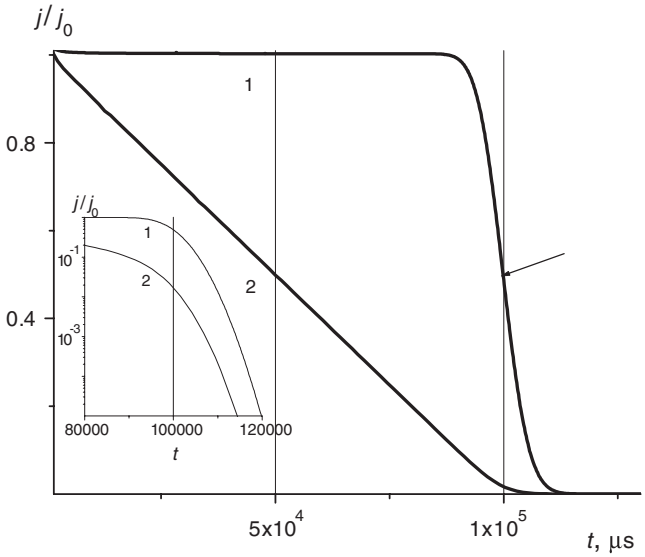

Figure 2. Calculated TOF (1) and TOF-2 (2) curves for Gaussian transport. Time of flight (marked by the arrow) is 0.1 s ($L = 10\ \mu$m, $F_0 = 1.33 \times 10^7$ V m^{-1}, $\tilde{\mu} = 7.5 \times 10^{-12}$ m^2 V^{-1} s^{-1} and $\tilde{D} = 1.87 \times 10^{-13}$ m^2 s^{-1}).

the Gaussian distribution 0.1 eV, prefactor ν being equal to the phonon frequency 10^{13} s^{-1}) the following MT parameters result: the trap distribution is the shifted one-sided Gaussian, $\mu_0 = 6.54 \times 10^{-9}$ m^2 V^{-1} s^{-1}, $\nu_0 = 4.54 \times 10^8$ s^{-1} and $\tau_0 = \nu_0^{-1}$. For 293 K, $\tilde{\mu} = 7.5 \times 10^{-12}$ m^2 V^{-1} s^{-1} and $\tilde{t} \approx 1.2$ ms. This value of $\tilde{\mu}$ has been used in figure 2.

3. Experimental technique

In our studies we rely heavily on pulse radiation sources but unlike early work (1975–80) with high energy electron accelerators (energy 3–9 MeV, fixed pulse length in the ns or μs range, dose rate easily changed between 10^6 and 10^9 Gy s^{-1}, single pulse operation mode [16]), the bulk of the experimentation starting from 1981 has been carried out using the electron gun ELA-50 [17].

This facility operates in a single pulse as well as truly continuous regimes. Electron energy can be easily adjusted from 3 to 65 keV so that both RIC and TOF techniques are readily realized by simply changing electron energy (the electron range at 65 keV is sufficiently large to ensure almost uniform irradiation of thin (up to 30 μm) polymer films). The pulse length (10 μs to 1 ms) and beam current density (up to 1 mA cm^{-2}) are easily made to order. The facility requires no special radiation shielding, takes only moderate room space and the researcher can sit by it during an experimental run.

We believe that electron guns are ideal instruments for the study of carrier transport. Spear [18], Gross *et al* [19] and Martin and Hirsch [20] have pioneered using electron guns as *universal* tools to probe charge carrier transport in conventional non-photoconductive dielectrics.

Also, an important advantage of an ionizing radiation (fast electrons in our case) is the possibility to exploit radiation chemistry results for assessing the concentration of free carriers escaping recombination in geminate pairs [21].

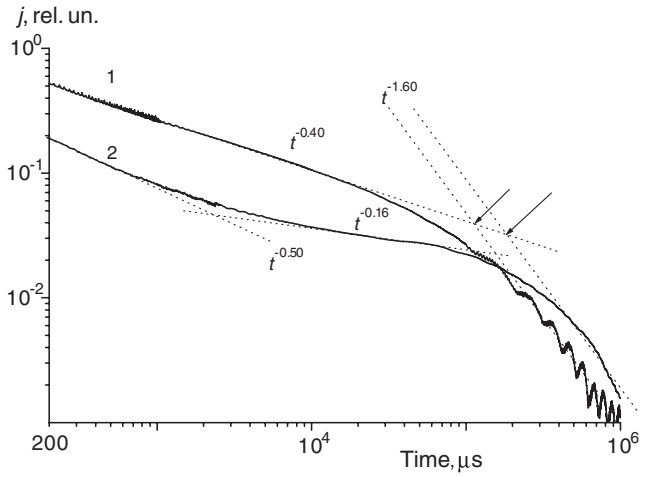

Figure 3. TOF-2 (1) and TOF (2) current transients in the same sample of PVK 20 μm thick. Experimental conditions: beam current density 10 μA cm^{-2}, electric field 1.6×10^7 V m^{-1}, pulse length 10 μs. The arrows indicate times of flight 110 (1) and 180 ms (2).

To obtain RIC and TOF data, which would allow an unequivocal interpretation, one needs to carry out measurements in the small signal regime so that the applied field remains unperturbed and no carrier loss to bimolecular recombination occurs. The current mode should be preferred. So, the *RC* time constant should be kept as small as possible. In general, a delicate compromise between numerous experimental factors (load resistor, beam current density, pulse length, irradiated area of the sample, applied electric field, etc) should be sought. Again, using fast electrons as the ionizing agent appreciably simplifies the task.

To improve the data collection and processing capability of the measuring circuit we have recently developed a computer assisted electronic scheme, which reads data points at a rate of 4×10^5 s^{-1} up to 10 s and stores them as a computer file to be processed by the Origin program. A printout is ready within minutes after an experimental run. It is important that this scheme has been made completely safe against breakdown of the sample.

Irradiation of polymer samples took place in a vacuum chamber ($\sim 3 \times 10^{-2}$ Pa) of the ELA-50 facility at room or elevated (up to 100 °C) temperatures.

Samples of PVK (Aldrich) were prepared on aluminium substrates 40 mm in diameter. The substrates were made from aluminium foil designed for offset printing plates to ensure a high adhesion of the polymer layer. Samples were prepared by casting a solution of PVK in chloroform or tetrachloroethane on a horizontal plate. All solvents were preliminarily purified by distillation. The substrates were washed in an ultrasonic bath with acetone. To prepare polymer layers with different thicknesses (10–35 μm), the concentration of the solution was varied from 50 to 120 mg ml^{-1}. When chloroform was used as a solvent, the layers were dried in a limited volume of air (under a Petri dish) to provide a low evaporation rate. After drying in air, the samples were placed in a vacuum chamber for at least 6 h. An aluminium top electrode 26 mm in diameter and 50–100 nm in thickness was thermally evaporated in a vacuum chamber at $\sim 5 \times 10^{-4}$ Pa.

4. Experimental results

Figure 3 presents experimental results obtained with both TOF variants on the same sample. Since the pulse length was 10 μs, current curves starting from 100 μs may be considered as

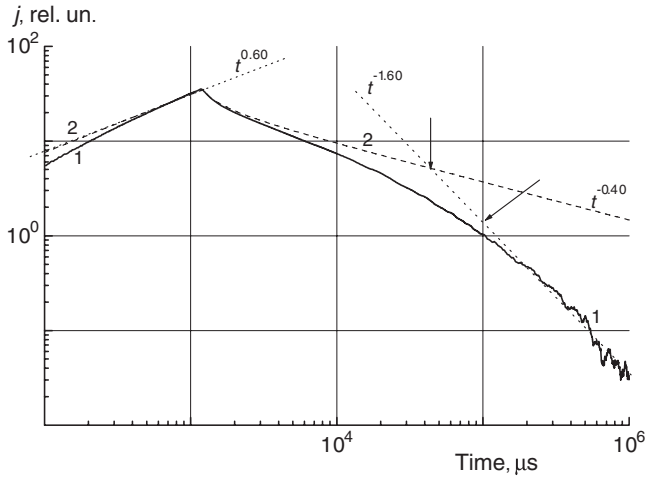

Figure 4. Experimental (1) and calculated (2) RIC curves in a PVK sample 24 μm thick at room temperature. Pulse length 1.25 ms, dose rate 500 Gy s^{-1}, electric field 2×10^7 V m^{-1}; the RIC at the end of the pulse per unit dose rate is 2.3×10^{-13} Ω^{-1} m^{-1} Gy^{-1} s ($RC = 20$ μs). Curve 2 has been computed for semi-infinite geometry (no transit effects). The vertical arrow marks the apparent transit time (44 ms) while the inclined one corresponds to the computed value for the δ-pulse irradiation ($\sim$100 ms). The build-up curve slightly deviates from its theoretical prediction partly due to *RC* distortion.

representing the PVK response to δ-pulse irradiation. The RIC current transient would then relate to the response to a rectangular excitation with the pulse length 1.25 ms (figure 4).

The fundamental result is that the TOF-2 transient fits very closely the predictions of the MT theory for $\alpha = 0.6$. The preflight ($j \propto t^{-1+\alpha}$) as well as postflight ($j \propto t^{-1-\alpha}$) asymptotes are clearly seen. It is particularly intriguing that the preflight asymptote extends for almost two decades, ensuring high accuracy of α determination. According to MT theory this asymptote runs as $j \propto t^{-1+\alpha-\eta}$, with $\eta \approx 0.01$ in this case. This is a direct consequence of the fact that holes begin to exit the sample at $t = 0$ (figure 1). This correction, though small, should be made in parameter fitting.

As expected, the shape of the preflight part of the TOF curve 2 on figure 3 unlike that of the TOF-2 is much more complicated. At early times it falls slightly faster ($\alpha \approx 0.5$) compared with TOF-2, then it slows down ($\alpha \approx 0.84$), making the determination of α uncertain. The post-transit part of the curve fits with theory rather well ($\alpha \approx 0.6$). As predicted, the TOF transit time exceeds that of TOF-2.

A note of caution is in order. Both current transients were highly reproducible. But whereas the TOF-2 signals displayed consistent uniformity among different samples within the same batch, the TOF preflight parts differed markedly, but we never observed a plateau, let alone a cusp. In all, nine samples have been tested in two different batches.

A very important observation is provided by figure 5, which shows that once an additional generation layer of Se has been applied to the PVK sample the TOF experiment reveals the presence of a well-defined plateau. The tail of the current is exceptionally long and at large times merges into $t^{-1.6}$ dependence, characteristic of the dispersive transport with $\alpha = 0.6$. The values of the equilibration time (4–8 ms) as well as of the drift mobility (1×10^{-11} m^2 V^{-1} s^{-1}) are surprisingly close to those of the Bassler model for PVK if the observed plateau is taken to mean its validity in this case. But this seems to be only a fortuitous coincidence. Indeed, preliminary measurements of the current-versus-voltage characteristic at the plateau revealed

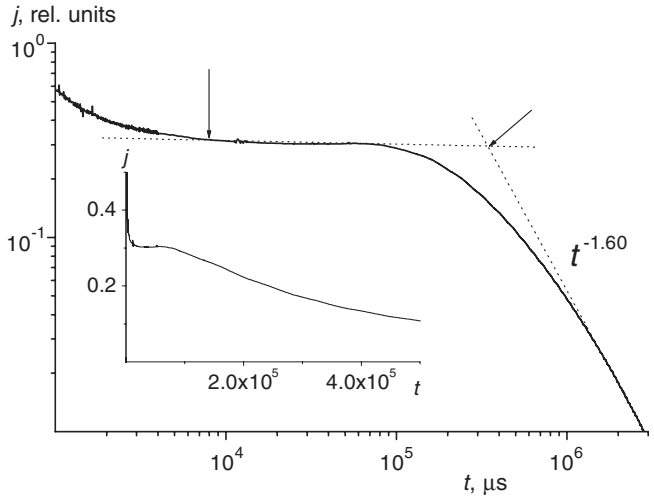

Figure 5. TOF curve in the PVK sample 13 μm thick supplied with a generation layer of Se ($\approx$1 μm). Electric field 1.2×10^7 V m^{-1}, small signal irradiation (the insertion gives the linear representation of the current transient).

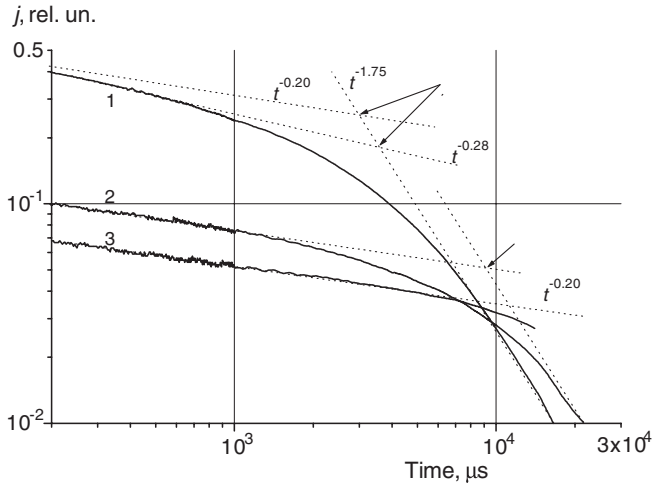

Figure 6. TOF-2 current transients in PVK at 353 K. Beam current density 0.31 (1, 2) and 3.1 μA cm^{-2} (3), applied voltage 480 (1), 240 (2) and 50 V (3). Sample thickness 28 μm, pulse length 10 μs. Transit times (indicated by arrows) 9.2 ms (2) and 3.0 or 3.6 ms (both refer to 1) depending on the approach used (the last figure is an upper limit).

exceptionally strong field dependence $j \propto F_0^{3.1}$, totally uncharacteristic of both simple TOF and TOF-2 ($j \propto F_0^{2.1}$) if measurements refer to the preflight signal region. Besides, contrary to these measurements in the case of the Se layer we saw very fast initial current decay $j \propto t^{-3.3}$ (not shown on the figure 5) due to the uncontrolled carrier drift in the generation layer. So, the presence of the latter seriously affects the shape of the current transient.

It is of great interest to estimate the extension of the dispersive stage of the relaxation in PVK. Room temperature experiments indicate that it is certainly larger than some seconds. To get a better estimate we used a high temperature experiment at 353 K (figure 6). Two

Table 1. Comparison of mobility data obtained by various authors at room temperature (all data have been reduced to $L = 10\ \mu$m and $F_0 = 2 \times 10^7$ V m^{-1}).

Mobility value (m^2 V^{-1} s^{-1})	Cited paper
1.7×10^{-11}	[7]
5.5×10^{-11}	[22]
6.0×10^{-12}	Present work

observations are important. First, it is seen that the dispersion parameter really rises, albeit to a slightly larger value (0.8 instead of 0.72) than the predicted $\alpha \propto T$ [1, 11]. Second, the achievement of Gaussian transport did not happen. This means that $\tilde{t}$ is much greater than 1 s at room temperature.

5. Data reduction

The fact that there are straight asymptotes on the TOF-2 curves in the $\log j - \log t$ representation is the most decisive single evidence against the Gaussian, and in favour of the dispersive, hole transport in PVK. The preflight asymptote follows a $t^{-1+\beta}$ law with β being constant to within 0.005 for at least two decades in time. It is the region of TOF-2 and RIC curves which experiences the least interference of surface traps as the majority of holes at this time are still in the bulk of the polymer away from both surface layers. So, this information relates directly to carrier behaviour in the bulk of the polymer and as such is most valuable.

We associate the exponent β with the dispersion parameter α of the MT theory, so that $\alpha = 0.60 \pm 0.01$ at room temperature. It has been shown that generally TOF-2 information allows determination only of the product $\mu_0\tau_0(\nu_0)^\alpha$ [13]. The best estimate based on transit times is 2.0×10^{-12} m^2/V s$^{0.6}$ and it is true to a factor of 1.5. As for individual factors, it may only be said that ν_0 is greater than $t_0^{-1} = 10^5$ s^{-1}.

Integration of TOF-2 curves gives the planar density of the transported hole charge, which in turn yields the value of the free ion yield $G_{\text{fi}} = 1.1 \pm 0.1$ at 2×10^7 V m^{-1} and room temperature. Using this value of G_{fi} and the TOF-2 current density at some point preceding the transit time [13], the above product was found to be 3.0×10^{-12} m^2/V s$^{0.6.}$. These two independent measurements show relatively good agreement.

To further separate the factors one needs to resort to model considerations (see below). We therefore set $\mu_0 = 1 \times 10^{-5}$ m^2 V^{-1} s^{-1} and adopt ν_0 (being the frequency of the retarded rotation of the pendant carbazole groups) equal to 2×10^6 s^{-1} at room temperature. For these values of μ_0 and ν_0, we obtain $\tau_0 = 3.9 \times 10^{-11}$ s. Note that the schubweg $\mu_0\tau_0 = 3.9 \times 10^{-16}$ m^2 V^{-1} is quite typical for quasi-band transport. RIC measurements (figure 4) confirm the above value of G_{fi} at the cited conditions. This completes the characterization of PVK at room temperature. Figure 7 illustrates our ability to fit the experimental TOF-2 data with MT theory. Also, at elevated temperature 353 K (figure 6, curve 1), the computed transit time 2 ms ($\nu_0 = 2.4 \times 10^7$ s^{-1}) compares favourably with the experimental value of 3 ms.

Now we would like to check the quality of PVK used in this work. The only way to do so is to compare the transit times reduced to some standard conditions (table 1).

It is seen that the quality of PVK used in the studies by Bos group is the highest. This is no wonder, as exceptional purification procedures have been employed. As a result, no traces of anthracene were found when it was analysed by absorption and high-performance liquid chromatography. Nevertheless, it is our samples that occasionally exhibited the highest value of $\alpha = 0.62$. The general MT theory shows that it is quite difficult to influence the dispersion parameter by the introduction of foreign traps, but once influenced the effect is conspicuous

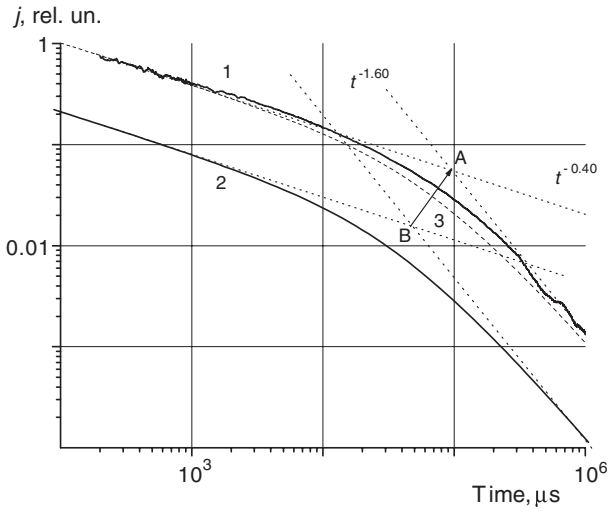

Figure 7. Experimental (1) and numerical (2 and 3) TOF-2 current transients in PVK at room temperature. The dashed curve (3) is curve 2 shifted along the vector $B\vec{A}$. Sample thickness 28 μm, electric field 2.6×10^7 V m^{-1}. Model parameters $\alpha = 0.6$, $\mu_0\tau_0 = 3.9 \times 10^{-11}$ m^2 V^{-1} and $\nu_0 = 2 \times 10^6$ s^{-1}. Curves 1 and 3 fit rather well.

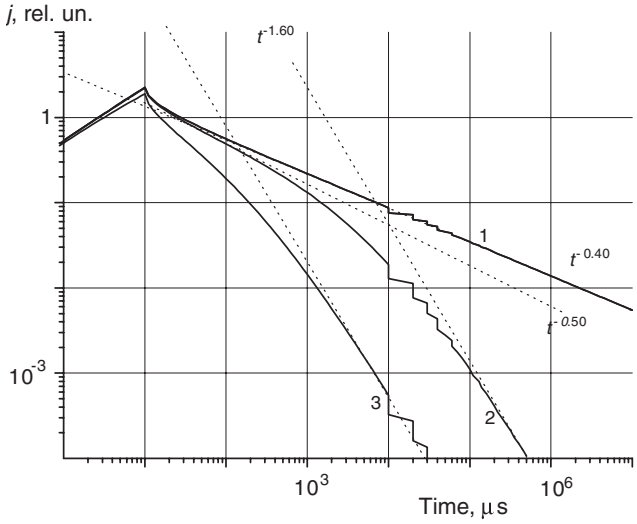

Figure 8. Calculated RIC curves illustrating the effect of introduction of foreign traps. Pulse length 10 μs, small signal irradiation. Capture rate by foreign traps: 0–10^7 (1), 10^8 (2) and 10^9 s^{-1} (3). Model parameters of the polymer: $\alpha = 0.6$, $\mu_0 = 10^{-5}$ m^2 V^{-1} s^{-1}, $\tau_0 = 0.39 \times 10^{-10}$ s and $\nu_0 = 2 \times 10^6$ s^{-1}, so that the capture rate by intrinsic traps $\tau_0^{-1} \approx 2.5 \times 10^{10}$ s^{-1}. For curve 2 the concentration of foreign traps is 4×10^{22} m^{-3} (the total concentration of intrinsic traps is 10^{25} m^{-3}). The change of initial slope by 0.1 is evident as well as fast transition to the decay law $t^{-1.6}$. Computation noise is seen around 10–50 ms.

(figure 8). Nothing of the kind has been observed. This proves that dispersive transport seems to be an intrinsic property of the *disordered* polymer itself and should not be ascribed to impurities inevitably present in it.

6. Model considerations

The GDM's inability to describe the RIC results in PVK [16] prompted us to look for an alternative explanation of disorder effects in such a way as to retain an overall MT formalism (ideally suited for treatment of the dispersive transport) while staying within the hopping conduction mechanism. Refer to [16, 23, 24] for details.

Unlike Bässler, we rely on the fluctuation free volume theory to account for the energy variation of hopping centres. The total concentration of the free volume microvoids in amorphous polymers is around 10^{25} m^{-3}, which is much less than the total concentration of hopping centres (3.8×10^{27} m^{-3} in PVK). These can be conveniently classified into two categories. One consists of the vast majority of sites, packed into a lattice identical to the real or hypothetical polymer single crystal. It serves as a transfer band to provide the microscopic hopping mobility $\mu_0 \approx 10^{-6}$–10^{-4} m^2 V^{-1} s^{-1}. Such a procedure is quite legitimate due to the existence of the short-range order as far as the first two coordination spheres of a homopolymer are concerned. And the few residual sites (<1%) are closely associated with microvoids. Exactly these sites may be presumed traps.

Trap energy variation is supposedly due to short-range interactions influenced by the microvoids' size. The resulting energy distribution is assumed exponential. To complete the formulation, one needs to specify the frequency factor. We identify it with the rotational rather than the translational diffusion of hopping centres. The frequency of retarded rotations of carbazole groups is around 2×10^6 s^{-1} at 293 K, with the activation energy 0.35 eV [25].

The electronic mobility in crystalline PVK has not been measured. Such data exist only for single crystals of its low molecular weight analogue—*N*-isopropylcarbazole: both carriers have a rather close mobility around 0.5×10^{-4} m^2 V^{-1} s^{-1} [26]. In parameter fitting we chose $\mu_0 \sim 10^{-5}$ m^2 V^{-1} s^{-1} as the molecular packing in PVK is slightly looser than in its analogue. Also, we would like to stress the ubiquity of the exponential trap distribution [16, 27]. One possible explanation is offered in [28], where it has been shown that states localized as a result of long wavelength potential fluctuations give rise to exponential band tails for three-dimensional random systems.

7. Discussion

We did not attempt measuring the field and thickness dependence of the transit time to increase the confirmative power of our approach. As indicated earlier, all existing theories predict a superlinear behaviour of the transit time as a function of the field, be it a power (MT) or a stretched exponential (PF) function as in [7]. The experimental method used is incapable of discerning which one of these is operative (figure 9).

The expected thickness dependence allows much more leeway. For dispersive transport $\hat{t}_{\rm tr} \propto L^{1.66}$ at room temperature while the alternative approach predicts a linear dependence. But again, we felt that quality measurements of this dependence were unattainable and these were not attempted. Nevertheless, a large wealth of existing data serves to substantiate the MT predicted dependence $\hat{t}_{\rm tr} \propto (L/F_0)^{1/\alpha}$ (see, for example, [1, 22, 29]).

Besides, it seems almost self-evident that once $j_{\delta v}(t)$ falls in time (the effective mobility is time dependent) the transit time is bound to depend on thickness superlinearly [1]. According to Hughes [30], in anthracene single crystal $j_{\delta v}(t)$ is really constant ($t \leqslant 400$ ns), in contrast to PVK exhibiting fast power-like decay.

But one interesting possibility should be mentioned. It concerns TOF curves in some polymers featuring a plateau and an abrupt current fall-off as reported in [31–34]. Such data may suggest some degree of equilibration. As already indicated in our earlier paper [35], it is imperative to put such polymers to TOF-2 scrutiny.

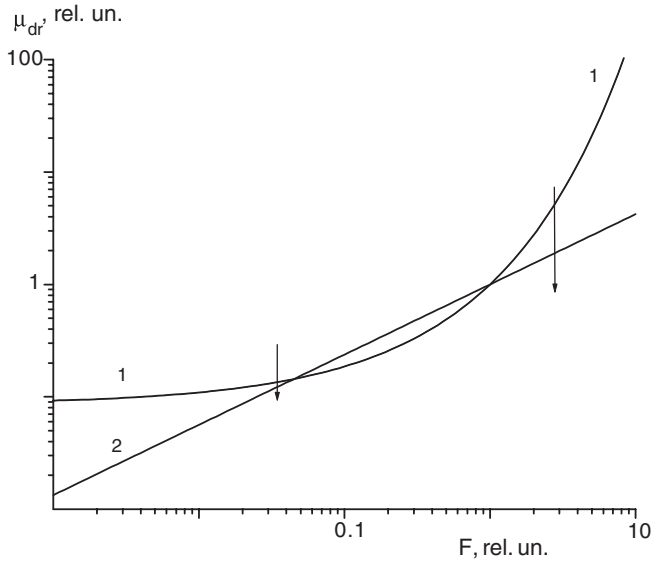

Figure 9. Field dependence of the drift mobility in PVK according to Gill's formula (1) [7] and MT theory for $\alpha = 0.6$ (2). The curves are made to coincide at $F = 1.0$ ($F = F_0/F^*$, where $F^* = 1.6 \times 10^7$ V m^{-1}). Arrows denote the range of fields normally used in the experiment.

Some comment concerning TOF generation-layer-assisted data is in order. The extensive investigations of Mort [8] are very helpful on this account. He used a 10 μs light pulse of $\lambda \approx 430$ nm to produce electron–hole pairs in a Se layer. The holes are then field driven to the Se–PVK interface and ultimately into PVK proper. Time-resolved TOF transients featured a cusp, which defined the transit time (a fastest transit time in the terminology of the author). It turned out that the field dependence of this transit time was extraordinary: $t_{\mathrm{tr}} \propto F_0^{-2.5}$. This adds to what has already been said in connection with figure 5 concerning the unusual effects a generation layer exerts on the TOF current shape. So, it seems only natural to recommend not using generation layers in studies of the charge carrier transport in order to avoid unnecessary complications.

It is noteworthy that according to [36] the exceptionally high mobilities of both charge carriers (about 1.5×10^{-2} cm^2 V^{-1} s^{-1}) at 3.8×10^6 V m^{-1} and 293 K found in disordered conjugated organometallic polymer networks (sample thickness 10 to 30 μm) do refer to the dispersive transport.

8. Conclusions

Hole transport in PVK, which may be regarded as a model disordered organic solid, is dispersive, in full accord with earlier investigations by researchers from Xerox and Eastman Kodak Research Centers (1970–1978) and contrary to the Gaussian disorder model. The best description of it is afforded by MT theory with the following set of field-independent parameters (room temperature): $\alpha = 0.60$, $\mu_0 = 10^{-5}$ m^2 V^{-1} s^{-1}, $\tau_0 = 3.9 \times 10^{-11}$ s, $\nu_0 = 2 \times 10^6$ s^{-1} (activation energy 0.35 eV). Free holes are generated in accordance with the Onsager mechanism ($G_{\mathrm{fi}} = 1.1$ at 2×10^7 V m^{-1}).

The TOF results are ambiguous and should be supplemented with TOF-2 measurements. Both methods show a close agreement as far as transit times are concerned but fundamentally

differ in registered waveforms, especially if an additional generation layer is used to enhance the TOF sensitivity. The TOF data suggest the possibility of the equilibration of the transport process, while the TOF-2 results strongly refute such a deduction. Unlike TOF-2, the classical TOF technique seems to suffer considerably from surface traps. Wide application of the TOF technique without any counterchecks resulted in the present controversial situation in the field of charge carrier transport in PVK.

To resolve this standing controversy, we resorted to a combination of two varieties of the TOF technique using both sheet-like and uniform carrier generation modes in conjunction with radiation-induced conductivity measurements. All three techniques were realized using an ELA-50 electron gun facility.

References

[1] Scher H and Montroll E W 1975 *Phys. Rev.* B **12** 2455
[2] Arkhipov V I, Iovu M S, Rudenko A I and Shutov S D 1979 *Phys. Status Solidi* a **52** 67
[3] Bässler H 1981 *Phys. Status Solidi* b **107** 9
[4] Bässler H 1993 *Phys. Status Solidi* b **175** 15
[5] Silver M, Dy K S and Huang I L 1971 *Phys. Rev. Lett.* **27** 21
[6] Pfister G and Scher H 1977 *Phys. Rev.* B **15** 2062
[7] Gill W D 1972 *J. Appl. Phys.* **43** 5033
[8] Mort J 1972 *Phys. Rev.* B **5** 3329
[9] Pfister G 1977 *Phys. Rev.* B **16** 3676
[10] Hummel A and Schmidt W F 1974 *Rad. Res. Rev.* **5** 199
[11] Rudenko A I and Arkhipov V I 1982 *Phil. Mag.* B **45** 189
[12] Arkhipov V I 1993 *J. Non-Cryst. Solids* **163** 274
[13] Tyutnev A P, Saenko V S and Pozhidaev E D 2004 *Polym. Sci.* B **48** 362
[14] Borsenbergen P M, Pautmeier L T and Bässler H 1992 *Phys. Rev.* B **46** 12145
[15] Plyukhin A V 1993 *Semiconductors* **27** 379
[16] Tyutnev A P 1996 *High Energy Chem.* **30** 1
[17] Tyutnev A P, Saenko V S, Pozhidaev E D and Akkerman A F 1982 *Phys. Status Solidi* a **73** 81
[18] Spear W E 1955 *Proc. Phys. Soc.* B **68** 991
[19] Gross B, Sessler G M and West J E 1974 *J. Appl. Phys.* **45** 2841
[20] Martin E H and Hirsch J 1972 *J. Appl. Phys.* **43** 1001
Hirsch J and Martin E H 1972 *J. Appl. Phys.* **43** 1008
[21] Hummel A 1974 *Adv. Rad. Chem.* **4** 1
[22] Bos F C, Guion T and Burland D M 1989 *Phys. Rev.* B **39** 12633
[23] Tyutnev A P, Sadovnichii D N, Saenko V S and Pozhidaev E D 2000 *Polym. Sci.* A **42** 10
[24] Tyutnev A P, Sadovnichii D N, Saenko V S and Pozhidaev E D 2001 *Chem. Phys. Rep.* **19** 1243
[25] Pochan J M, Hinman D F and Nash R 1975 *J. Appl. Phys.* **46** 4115
[26] Sharp J H 1967 *J. Phys. Chem.* **71** 2587
[27] Monroe D and Kastner M A 1986 *Phys. Rev.* B **33** 8881
[28] Soukoulis C M, Cohen M H and Economou E N 1984 *Phys. Rev. Lett.* **53** 616
[29] Mort J, Pfister G and Grammatica S 1976 *Solid State Commun.* **18** 693
[30] Hughes R C 1971 *IEEE Trans. Nucl. Sci.* **18** 281
[31] Abkowitz M A, Facci J S, Limburg W W and Yanus J F 1992 *Phys. Rev.* B **46** 6705
[32] Stolka M, Yanus J F and Pai D M 1984 *J. Phys. Chem.* **88** 4707
[33] Borsenbergen P M, Pautmeier L T and Bässler H 1993 *Phys. Rev.* B **48** 3066
[34] Borsenbergen P M, Pautmeier L T, Richert R and Bässler H 1992 *J. Chem. Phys.* **94** 8276
[35] Tyutnev A P, Saenko V S, Kolesnikov V A and Pozhidaev E D 2005 *High Perform. Polym.* **17** 175
[36] Kokil A, Shiyanovskaya I, Singer K D and Weder C 2002 *J. Am. Chem. Soc.* **124** 9978